SPRI: Simulator of Polarimetric Radar Images

R. D. De Roo, J. Munn, L. E. Pierce, A. Y. Nashashibi, F. T. Ulaby
Dept. of Electrical Engineering and Computer Science
The University of Michigan
Ann Arbor, MI 48109-2122 USA
email: lep@eecs.umich.edu
and
G. S. Samples
Army Research Laboratory
Adelphi, MD 20783 USA

ABSTRACT

SPRI consists of a suite of image processing programs for producing realistic millimeter-wave (MMW) radar images artificially on a workstation. The heart of the simulation approach is a polarimetric Rayleigh clutter simulator coupled to a clutter database. The simulator produces high resolution single-look polarimetric images. Hard targets can then be embedded into this clutter map, and the resultant image can be degraded in resolution, number of looks, polarization, etc. to match that which would be observed by a real sensor. Examples of simulated images, and comparisons of these simulations to actual images, are presented.

The MMW Clutter Database is the most comprehensive to-date database of over 3500 Mueller matrices for many kinds of terrestrial clutter measured at 35 and 95 GHz, many of which are at incidence angles close to grazing. The database can be accessed via a World Wide Web flexible interface that enables data to be combined in new and unique ways specified by the user, and displayed in either tabular or graphical format. The structure and access procedure to the database are described.

*Prepared through collaborative participation in the Advanced Sensors Consortium sponsored by the U.S. Army Research Laboratory under the Federated Laboratory Program, Cooperative Agreement DAAL01-96-2-0001.

1. INTRODUCTION

Radar images have proven to be invaluable tools in the remote sensing community, with regard to both civilian and military applications. With the advent of Synthetic Aperture Radar (SAR), very high resolution images can be readily generated at both centimeter and millimeter wavelengths. For many tasks, such as testing Automatic Target Recognition (ATR) algorithms, it is desirable to have a particular radar image taken with a particular sensor under particular conditions. Such radar images are often unavailable, due to the fact that a radar observation like the one desired has never been performed, or because an existing image cannot be released. To make the observation would be very expensive, and even more so if the sensor has yet to be built.

Not all applications require real images. Training of personnel to read radar images, for example, do not require real images. The aforementioned ATR testing is another example where real images are not required. Evaluation of proposed sensors prior to prototyping is another application of synthesized imagery. This document describes the techniques for radar image simulation using SPRI, the Simulator of Polarimetric Radar Images.

The majority of any radar image consists of clutter. Clutter behaves according to a particular statistical distribution, and the first section of this paper explores the ways of describing that distribution with the Rayleigh distribution. Then, a generalization of this distribution is made to the polarimetric case, and the algorithm for generating Rayleigh-distributed polarimetric data is given. Remaining objects in an image consist of man-made targets which may or may not behave like clutter does. Polarimetric clutter simulation is combined with existing target embedding techniques.

The clutter generation depends on two parts: a clutter database and a simulation algorithm. The simulation algorithm converts random numbers into complex scattering matrices, $\mathbf{S}$, which are statistically appropriate for the clutter being modeled. But the conversion requires information on the covariance of the $\mathbf{S}$ matrix elements that is unique to the particular clutter being modeled. A clutter database of measured Mueller matrices for various types of clutter under different conditions provides the information required for the simulator algorithm.

Several radar image simulators ([1–3] for example) have been introduced, and very many collections of radar data of terrain have been published ([4–10] for some examples). This paper documents a simulator of radar images for terrain at millimeter wavelengths, coupled with an online database of measurements of carefully selected homogeneous clutter. All of these measurements in the Clutter Database are at millimeter wavelengths and are fully polarimetric.

2. CLUTTER AND THE RAYLEIGH DISTRIBUTION

For this simulator to function realistically, the statistical nature of clutter must be accurately characterized. We found that the Rayleigh model for fading is appropriate for clutter which is homogeneous, and that inhomogeneous clutter can be described as a collection of homogeneous clutter but with varying normalized radar cross section (RCS) [11]. Thus, the most general type of clutter can be generated using the Rayleigh model, to account for the fading, coupled with the Bayes rule, to account for the variations in the normalized RCS.

This section summarizes the conclusions found in [11]. That study investigated the statistical nature of clutter observed near grazing incidence and at 95 GHz for three specific cases of clutter: bare ground, snow cover over a bare ground, and a heterogeneous scene containing bare ground, trees, bushes, and tall grasses. The bare ground constitutes homogeneous clutter under homogeneous conditions and the magnitude of the amplitude is Rayleigh distributed. While the snow cover is homogeneous clutter, the conditions under which it was observed are heterogeneous, and the Bayes rule is employed to describe the clutter distribution. The Bayes rule integrates variations due to signal fading with the underlying variations in the backscattering coefficient associated with the heterogeneity. The heterogeneous scene is also successfully described

with the Bayes rule.

For the purpose of furthering discussion, let us establish a nomenclature of the scattering process and describe its statistical nature. Assume a polarimetric radar image of homogeneous terrain consists of a large number of pixels, N, each of area A. For each pixel, the backscatter measured by the system is in the form of the scattering matrix $\mathbf{S}$, where [12]:

$$\mathbf{S} = \begin{bmatrix} S_{vv} & S_{vh} \\ S_{hv} & S_{hh} \end{bmatrix}. \tag{1}$$

The elements of $\mathbf{S}$ are the complex scattering amplitudes associated with the four different combinations of transmit and receive linear polarizations. Element S, where S represents any one of S_{vv}, S_{vh}, S_{hv} or S_{hh}, may be expressed as

$$S = S' + j\ S'' = |S| e^{j\phi}, \tag{2}$$

where $S' = \mathrm{Re}[S], S'' = \mathrm{Im}[S], |S|$ is the magnitude of S and ϕ is its phase angle. The joint probability density function of the real and imaginary parts of S are each Gaussian distributed with zero means and equal variances and is given by

$$p(S', S'') = \frac{1}{2\pi s^2} \exp\left[-\left(S'^2 + S''^2\right)/2\ s^2\right] \tag{3}$$

where s is the standard deviation.

The pdf of $V = 2\sqrt{\pi}|S|$ is given by

$$p(V \mid \bar{V}) = \frac{\pi}{2}\ \frac{V}{\bar{V}^2} \exp\left[-\frac{\pi}{4}(V/\bar{V})^2\right], \quad V \geq 0, \tag{4}$$

where $\bar{V}$ is the mean value of V and it is related to the standard deviation s by $\bar{V} = \sqrt{\frac{\pi}{2}}(2\sqrt{\pi}\ s) = \sqrt{2}\pi s$. The term "Rayleigh fading" is used to describe the scattering process for any quantity associated with statistically homogeneous clutter, even though it is only the received voltage magnitude that is Rayleigh distributed while the distributions of the backscattered power and other quantities are not. For intensity (power) or intensity related quantities, such as the radar cross section per unit area when expressed in units of $(\mathrm{m}^2/\mathrm{m}^2)$, the pdf for a single sample drawn from a population with mean $\bar{I} = \frac{4}{\pi}\bar{V}^2$ becomes an exponential [4, 13]:

$$p(I \mid \bar{I}) = \frac{1}{\bar{I}} \exp\left[-I/\bar{I}\right], \quad I \geq 0 \tag{5}$$

where $\bar{I}$ is the mean value of I and $I = V^2 = 4\pi|S|^2$. If a scene with varying $\bar{I}$ was imaged by a one-look per pixel radar, the observed intensity of the resultant speckled radar image would be characterized by a pdf given by the Bayes rule as [14]:

$$p(I) = \int_0^\infty p(I \mid \bar{I})\ p(\bar{I})\ d\bar{I} \tag{6}$$

where $\bar{I}$ is the mean intensity (in linear units of $\mathrm{m}^2/\mathrm{m}^2$), and $p(\bar{I})$ is the pdf of the mean intensities which vary from region to region in a typical radar image. To apply this Bayes formula, we shall convert the integral into a summation over observed mean values for homogeneous clutter under homogeneous conditions. If we denote by $\bar{I}_k$ the mean value obtained by averaging many independent samples of homogeneous clutter, as would be contained in the Clutter Database, then (6) may be rewritten as

$$p(I) = \frac{1}{N_0} \sum_{k=1}^{N_0} \frac{1}{\bar{I}_k} \exp(-I/\bar{I}_k) \tag{7}$$

where we have replaced $p(I \mid \bar{I})$ with the exponential pdf given by (5).

For linear detection, the equivalent expressions are

$$p(V) = \int_0^\infty p(V \mid \bar{V})\, p(\bar{V})\, d\bar{V} \tag{8}$$

for the continuous case, and

$$p(V) = \frac{\pi}{2N_0} \sum_{k=1}^{N_0} \frac{V}{\bar{V}_k^2} \exp\left[-\frac{\pi}{4} \left(\frac{V}{\bar{V}_k} \right)^2 \right] \tag{9}$$

for the discrete case.

In our previous work [11], we compared the distributions presented in this section with those obtained from measurements made by the Army Research Laboratory [9] as part of the Smart Weapons Operability Enhancement project [15].

We confirmed that the Rayleigh fading model is quite suitable for characterizing the backscatter distribution for homogeneous terrain under homogeneous conditions, and we demonstrated that the Bayes formula provides a physically based approach for characterizing the distributions for heterogeneous terrain. As a result, a comprehensive database of clutter measurements of homogeneous terrain should be sufficient for generating simulated radar images of heterogeneous scenes.

3. THE CLUTTER DATABASE

We have collected a Clutter Database of many polarimetric measurements of the Mueller matrix of terrain at millimeter-wave (MMW) frequencies and at near grazing incidence. Each of these measurements represents an average over many independent samples of homogeneous clutter under homogeneous conditions. In addition to the Mueller matrix, we have included in the Clutter Database extensive ground truth so that models for the radar backscatter may be generated from the data taking into account the underlying physical parameters which control the backscatter. These models, or the data itself, can be used to model not only homogeneous clutter under homogeneous conditions, but also under heterogeneous conditions, as outlined in the previous section. The next section describes in detail how this is done polarimetrically.

The Clutter Database is an online repository for calibrated polarimetric backscatter measurements. As of January 2001, the Clutter Database contains over 3500 Mueller matrices measured at Ka- and W-bands. Most of this data is in an angular range near grazing, but some measurements exist at nearly all angles of incidence. All of the data is fully polarimetric, and therefore the backscattering coefficient values are available not only in the linear basis (VV, HH, and HV polarizations) but also in the circular basis (LL, RR, and LR polarizations).

The Clutter Database is a growing, living entity. In addition to ongoing MMW measurements being conducted at the University of Michigan, previous polarimetric backscatter measurements at other frequencies (such as L-, C- and X-bands) may also someday be included in the Clutter Database. In principle, other measurements of clutter, such as bistatic measurements, measurements of extinction within scattering media, or RCS measurements of hard targets could become part of the Clutter Database.

3.1. Measurement System Description

The fully polarimetric ultra-fast wideband millimeter-wave scatterometer system, developed at The University of Michigan, was used in conducting the majority of these measurements. The system consists of two RF-frontend units (one at 35 GHz

and the other at 95 GHz) and an IF transceiver (transmit/receive) module. The scatterometer system operates in Real Aperture Radar mode (RAR) with an angular resolution of 2 and 1.4 degrees at 35 and 95 GHz respectively. In addition, the two scatterometers have 1 foot range resolution (500 MHz systems).

The principle of operation of the ultra-fast scatterometer system can be summarized as follows: The transceiver module generates a C-band pulse chirped over 500 MHz. The chirped pulse is upconverted in the RF-frontend units to the desired MMW frequencies and transmitted as either a vertically or horizontally polarized pulse. The backscattered response, intercepted by the receive antenna, is downconverted in the RF-frontend units to C-band and sent back to the IF transceiver module. Inside the transceiver, the received signal is downconverted once again to baseband and detected directly using a Digitizing Oscilloscope. The data is then transferred to a personal computer where the time domain response and/or the frequency domain response of the target (or clutter) under test can be extracted. An important feature of this system is the high speed with which it acquires the complete scattering matrix, thereby preserving phase coherence between polarizations. Details about this system may be found in [16].

3.2. Other Sources of Data

The University of Michigan has attempted to collect polarimetric MMW data from as many sources as possible for inclusion in the Clutter Database. The Clutter Database includes numerous measurements collected since 1991 with a network analyzer-based scatterometer system [17] designed and built by the University of Michigan.

Other sources of data include clutter measured by the Army Research Laboratory with their polarimetric W-band mono-pulse radar [18] as part of the Smart Weapons Operability Enhancement (SWOE) program [9], and measurements of clutter by the University of Massachusetts at 35, 95 and 225 GHz [6].

3.3. Accessing the Clutter Database

The Clutter Database is available online free of charge but it is password protected. A password can be obtained by an institution (University or corporation) in a country which is part of NATO when a letter of need is received at the University of Michigan from the institution's government sponsor, or from the Army Research Laboratory. Contact the authors at the email address listed for detailed information on accessing the Clutter Database.

A brief overview of the contents of the Clutter Database is available at
http://larch.eecs.umich.edu/∼deroo/clutterhelp
This World Wide Web site is not password protected.

QueryBuilder, the generic web interface to an SQL database, and the Clutter Database in particular, is located at
http://larch.eecs.umich.edu/cgi-bin/querybuilder/querybuilder.cgi
but requires a password for access to the Clutter Database. A description of QueryBuilder's capabilities, and several examples of queries of the Clutter Database, can be found at
http://larch.eecs.umich.edu/cgi-bin/querybuilder/querybuilderhelp.cgi
This World Wide Web site is also not password protected.

3.4. Clutter Database Structure

The database is written in Structured Query Language (SQL), a multi-vendor supported database language. SQL describes an industry standard for communicating with databases, and SQL supports many kinds of fast conditional searches of a database.

The WWW interface to the database, known as QueryBuilder, simply mimics the syntax of the 'Select' query, the command for extracting information from an SQL-compatable database. In addition to the QueryBuilder help page, details on the construction of 'Select' queries can be found from numerous books ([19, 20], for example).

The particular variant of SQL used for the Clutter Database is MySQL, a free software package optimized for speed and robustness. MySQL is not completely compatible with the ANSI SQL92 standard, but the incompatible features of MySQL have been avoided in its implementation for the Clutter Database.

The database consists of a number of files, each of which, in the parlance of SQL, constitutes a table.

The main table is denoted the Mueller table, and it contains not only the Mueller matrix data but all the parameters in Table 1. The date and time are included in all tables. In fact, they jointly constitute the primary key in each table (that is, they must be unique for each entry and can be used to index the entries) and can be used to cross reference data in the tables.

The Clutter Database consists of multiple tables. The main table is the 'mueller' table, which contains the measured Mueller matrices of clutter for many kinds of terrain under many conditions. The mueller table contains the following groups of information:

1. acquisition (date and time of the measurement, the organization which acquired the data, the organization which paid for the data, etc.),
2. radar parameters (center frequency, band designation, bandwidth, angle of incidence, etc.),
3. radar return (the Mueller matrix elements, σ^0 in linear and circular basis, phase difference statistics, etc.), and
4. clutter classification (target classes, roughness, wetness, species names, etc.).

In addition to the main table, there are the ancilliary information tables and the ground truth tables. The ancilliary information tables supplements the mueller table information on the radar systems; the ground truth tables supplements the mueller table information on the clutter classes. In both cases, the records in these tables are cross-indexed to the mueller table via the time and date of the radar measurement, as this is (nearly) a unique key for the data.

Presently, two tables contain the ancilliary data for two types of sensor configurations available at the University of Michigan for the measurements. The UFWBR table, for the Ultra-Fast Wide-Band Radar sensor, and the NWA table, for the Network Analyzer-based radar sensor, contain data about the measurement which are intended to be used primarily by the University of Michigan staff for data verification.

Several additional tables contain detailed ground truth measurements, the names of which each start with "gt_." Examples of these tables include gt_alfalfa, gt_corn, gt_grass, gt_snow, gt_soybean, gt_surface, and gt_tree.

To facilitate a detailed description of the contents of the mueller table and the ancilliary and ground truth tables, a relatively small table called 'HELP' contains a description of the column names for each table and meaning of the data contained therein.

Column	variable type	units	meaning
time_msmt	time	HH:MM:SS	Time of Measurement
date_msmt	date	DDMMYYYY	Date of Measurement
rf_ctr	real	GHz	sensor center frequency
rf_bw	real	GHz	RF bandwidth (GHz)
targ_type	char(5)	point|distr|other	target type
descript	varchar(32)		field description of target
pts_indep	real		est number of independent samples
msmt_mode	char(32)	NWA|UFWBR	sensor
ang_dep	real	deg	depression angle
ang_graz	real	deg	grazing angle
ang_inc	real	deg	incidence angle (90-ang_graz)
ang_look	real	deg	look angle (90-ang_dep)
m11	real	(see below)	avg modified mueller matrix
⋮			
m44	real		
sig_vv	real	dB or dBsm	sigma VV polarization
sig_hh	real	dB or dBsm	sigma HH polarization
sig_lx	real	dB or dBsm	sigma lin. cross polarization
sig_ll	real	dB or dBsm	sigma LL polarization
sig_rr	real	dB or dBsm	sigma RR polarization
sig_cx	real	dB or dBsm	sigma circ. cross polarization
sigma_units	char(5)	RCS|sigma0	sigma type
alpha_c	real		copol correlation
zeta_c	real	deg	copol mean phase difference
alpha_x	real		crosspol correlation
zeta_x	real	deg	crosspol mean phase difference
targ_class	char(12)		clutter type code
spec_dom_lat	varchar(16)		dominant species Latin name
spec_dom_com	varchar(16)		dominant species common name
targ_site	varchar(16)		address of measurement site
photo_host	char(8)		host system for photos
photo_path	char(32)		path to photo directory
photo_file	char(12)		list of photo files
targ_comm	varchar(32)		target comments

Table 1: Fields of the Mueller table.

3.5. The Mueller Matrix

The modified Mueller matrix (hereafter known as the Mueller matrix) is given by

$$\mathbf{M} = \begin{bmatrix} M_{11} & M_{12} & M_{13} & M_{14} \\ M_{21} & M_{22} & M_{23} & M_{24} \\ M_{31} & M_{32} & M_{33} & M_{34} \\ M_{41} & M_{42} & M_{43} & M_{44} \end{bmatrix} =$$

$$\begin{bmatrix} \left\langle |S_{vv}|^2 \right\rangle & \left\langle |S_{vh}|^2 \right\rangle & \langle \Re e\{S_{vh}^* S_{vv}\} \rangle & -\langle \Im m\{S_{vh}^* S_{vv}\} \rangle \\ \left\langle |S_{hv}|^2 \right\rangle & \left\langle |S_{hh}|^2 \right\rangle & \langle \Re e\{S_{hh}^* S_{hv}\} \rangle & -\langle \Im m\{S_{hh}^* S_{hv}\} \rangle \\ 2\langle \Re e\{S_{vv} S_{hv}^*\} \rangle & 2\langle \Re e\{S_{vh} S_{hh}^*\} \rangle & \langle \Re e\{S_{vv} S_{hh}^* + S_{vh} S_{hv}^*\} \rangle & \langle \Im m\{S_{vh} S_{hv}^* - S_{vv} S_{hh}^*\} \rangle \\ 2\langle \Im m\{S_{vv} S_{hv}^*\} \rangle & 2\langle \Im m\{S_{vh} S_{hh}^*\} \rangle & \langle \Im m\{S_{vv} S_{hh}^* + S_{vh} S_{hv}^*\} \rangle & \langle \Re e\{S_{vv} S_{hh}^* - S_{vh} S_{hv}^*\} \rangle \end{bmatrix} \tag{10}$$

and is a complete description of polarimetric scattering behavior for statistically homogeneous clutter. The symbol $\langle\rangle$ denotes ensemble averaging. The form of the Mueller matrix arises from the fact that the modified Stokes vector, which describes the intensity and polarization state of an electromagnetic wave, representing a wave incident on clutter, is transformed by matrix multiplication with the Mueller matrix into the appropriate modified Stokes vector representing the wave scattered from the clutter. The expression above is valid for both the Forward Scattering Alignment (FSA) and the Backscattering Alignment (BSA) conventions, however, as the $\mathbf{S}$ matrix is defined differently in these conventions, a given Mueller matrix full of numbers must be specified as to which alignment is used. The Clutter Database uses the BSA convention. The interested reader is referred to Ulaby and Elachi [12] for a complete treatment of these topics.

4. THE SIMULATOR ALGORITHM

This section describes a recipe for repeatedly finding random values for the $\mathbf{S}$ matrix which are statistically correct for a particular homogeneous clutter. That is, the $\mathbf{S}$ elements are individually Rayleigh distributed but which together satisfy a particular Mueller matrix. The algorithm approach is found in an appendix to an article by Lee, *et al.* [21].

4.1. Simulating Scattering Matrices from a Mueller Matrix

Let us describe the scattering matrix $\mathbf{S}$, given by (1), as a vector:

$$\mathbf{z} = \begin{bmatrix} S_{hh} \\ S_{vv} \\ S_{hv} \end{bmatrix} \tag{11}$$

Then, the covariance matrix $\mathbf{C}$ is given by $\mathbf{C} = \left\langle \mathbf{z}\, \mathbf{z}^\dagger \right\rangle$ (where $\mathbf{z}^\dagger$ indicates the conjugate transpose of $\mathbf{z}$), or, explicitly,

$$\mathbf{C} = \begin{bmatrix} \left\langle |S_{hh}|^2 \right\rangle & \langle S_{hh} S_{vv}^* \rangle & \langle S_{hh} S_{hv}^* \rangle \\ \langle S_{vv} S_{hh}^* \rangle & \left\langle |S_{vv}|^2 \right\rangle & \langle S_{vv} S_{hv}^* \rangle \\ \langle S_{hv} S_{hh}^* \rangle & \langle S_{hv} S_{vv}^* \rangle & \left\langle |S_{hv}|^2 \right\rangle \end{bmatrix}. \tag{12}$$

This representation of the polarimetric backscatter is a simple rearrangement of the information contained in the Mueller matrix, which is stored in the Clutter Database.

For Rayleigh distributed scattering, the covariance matrix is sufficient to describe the distribution of the $\mathbf{S}$ matrix, with the joint pdf of the $\mathbf{S}$ matrix elements given by [22]:

$$p(\mathbf{z}) = \frac{1}{\pi^3 |\mathbf{C}|} \exp\Big(-\mathbf{z}^\dagger \cdot \mathbf{C}^{-1} \cdot \mathbf{z}\Big) \tag{13}$$

This equation is a polarimetric generalization of (3).

If we do an eigen analysis on the covariance matrix, we can express it as

$$\mathbf{C} = \mathbf{V} \cdot \mathbf{\Lambda} \cdot \mathbf{V}^{-1} \tag{14}$$

where $\mathbf{\Lambda}$ is the diagonal matrix consisting of the real eigenvalues of the Hermitian matrix $\mathbf{C}$, and $\mathbf{V}$ is a matrix consisting of the properly ordered eigenvectors of $\mathbf{C}$. Since each eigenvector can be arbitrarily scaled, a scaling which makes $\mathbf{V}$ unitary is chosen, so that $\mathbf{V}^{-1} = \mathbf{V}^\dagger$ and $|\mathbf{V}| = 1$ [23]. Then, it is possible to express the distribution as

$$\begin{aligned} p(\mathbf{z})d\mathbf{z} &= \frac{1}{\pi^3 |\mathbf{C}|} \exp\Big(-\mathbf{z}^\dagger \cdot \mathbf{V} \cdot \mathbf{\Lambda}^{-1} \cdot \mathbf{V}^{-1} \cdot \mathbf{z}\Big) d\mathbf{z} \\ &= \frac{1}{\pi^3 |\mathbf{\Lambda}|} \exp\Big(-\mathbf{y}^\dagger \cdot \mathbf{I} \cdot \mathbf{y}\Big) d\mathbf{z} \\ &= \frac{1}{\pi^3} \exp\Big(-\mathbf{y}^\dagger \cdot \mathbf{y}\Big) d\mathbf{y} = p(\mathbf{y})d\mathbf{y} \end{aligned} \tag{15}$$

where $\mathbf{I}$ is the identity matrix,

$$\mathbf{z} = \mathbf{V} \cdot \mathbf{\Lambda}^{\frac{1}{2}} \cdot \mathbf{y} \tag{16}$$

and $\mathbf{\Lambda}^{\frac{1}{2}}$ is the diagonal matrix of square roots (arbitrary branch) of the eigenvalues of $\mathbf{C}$.

The pdf of $\mathbf{y}$, as given by the last equality of (15), is the pdf of 3 independent complex Gaussian random variables, each with zero mean and unit variance. Such Gaussian random variables are easily obtained [24]. Thus, (16) suggests that the appropriate linear combination of a set of 3 independent complex Gaussian random variables can give the elements of the $\mathbf{S}$ matrix which has the properties of the desired Mueller matrix. The $\mathbf{S}$ matrix generation algorithm is, therefore, as follows:

First, make many individual measurements (via SAR or scatterometer) of the particular clutter type under the desired conditions. Each measured $\mathbf{S}$ matrix is converted to a Mueller matrix and all of these Mueller matrices are averaged together to form a single "average Mueller matrix" which represents the statistical polarimetric characteristics of that clutter. This information is stored in the Clutter Database. This process is depicted in the top portion of the flow chart in Fig. 1.

For simulation, we must identify a region in an image as a particular clutter type. Then, the appropriate average Mueller matrix is extracted from the Clutter Database. This Mueller matrix is converted to a covariance matrix, and this covariance matrix is decomposed into a unitary matrix of eigenvectors and a diagonal matrix of square roots of the eigenvalues. This process is portrayed in the middle of Fig. 1 with single headed arrows.

A random number generator is then employed to create three independent zero-mean unit-variance complex Gaussian random numbers for each pixel in the image region. These random numbers are linearly combined according to (16) to create the simulated $\mathbf{S}$ matrix values. Figure 1 shows this process towards the bottom with double headed arrows.

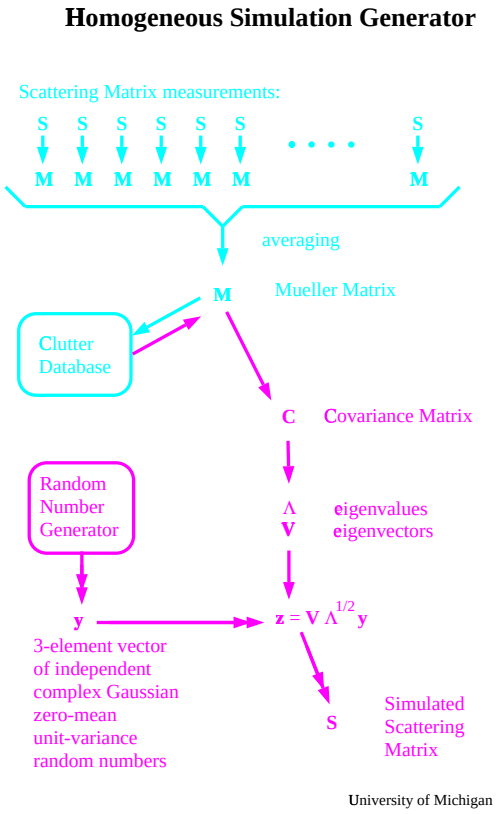

Figure 1: Flow diagram for the Simulation algorithm.

For the next *pixel* in the image region, the algorithm repeats starting with the random number generator. Since the average Mueller matrix is the same across the region, we do not need to calculate new eigenvalues or eigenvectors. That is, subsequent pixels in a region involve only the process shown in Figure 1 with double headed arrows.

For the next *region* in the image, a new average Mueller matrix appropriate for the clutter in this next region must be extracted from the Clutter Database. That is, the first pixel of each region involves the entire process shown in Figure 1 (i.e. the middle and bottom portions of the flow chart).

If we subdivide the area for a particular clutter type in the image to be simulated into appropriately interleaved regions, for which the conditions differ slightly, we can simulate texture and non-Rayleigh fading statistics, much like that for the snow discussed earlier.

5. EXAMPLES OF SIMULATED IMAGES

By homogeneous simulation it is meant that the image is broken up into regions, and each region contains Rayleigh clutter that can be described by a single Mueller matrix. This is a major assumption about the nature of the data observed, but we shall see that this is adequate for using SPRI as a lossy SAR image compression algorithm. Further use of this assumption

Figure 2: Single look Ka-band SAR image used for verifying the homogeneous simulation algorithm of SPRI. HH is in red, VV is in green and HV is in blue. The depression angle is 3.8° and illumination is from the left. Trees in the upper left of the image are casting long shadows across the image.

Figure 3: Aerial photo of region in the previous figure. This photograph and the image in the previous Figure are not co-registered. The bands across the photo are artifacts.

is made in the subsequent subsections where a SAR image is simulated from an aerial photograph and where a SAR image at Ka-band is used to simulate the same scene at W-band.

The imagery used was obtained by the Lincoln Lab 33.6 GHz SAR [25, 26] on behalf of the Army Research Laboratory. The image is one frame of many acquired near Hillsboro, MD, on the Eastern Shore, about 50 km East of Annapolis, MD, in the Spring of 1992. The particular image considered here is from mission 335, pass 5, level 4, frame 216. It has 2048 pixels in the range direction and 512 pixels in the azimuth direction; pixel resolution is 22.87 cm in both directions. The data are single look complex and fully polarimetric. This image is shown in Figure 2, and an aerial photograph of the same area taken at about the same time is shown in Figure 3.

5.1. A Fidelity Test: Simulation as a Lossy Compression

The first image simulated will demonstrate two features of the most basic parts of SPRI: first, it will show how the algorithm displayed in Figure 1 is implemented, and second, it will show how faithful the simulation algorithm is in re-creating real data.

The first step is to segment the image into regions of reasonable homogeneity. This was achieved by converting the VV, HH, and VH amplitude channels to decibels, so that the fading variation would be constant across the image [27], and successively applying an enhanced Lee adaptive despeckling filter [28] on each of these channels. The resulting despeckled channels were used as the input to an unsupervised clustering algorithm [29] the output of which was sieved to

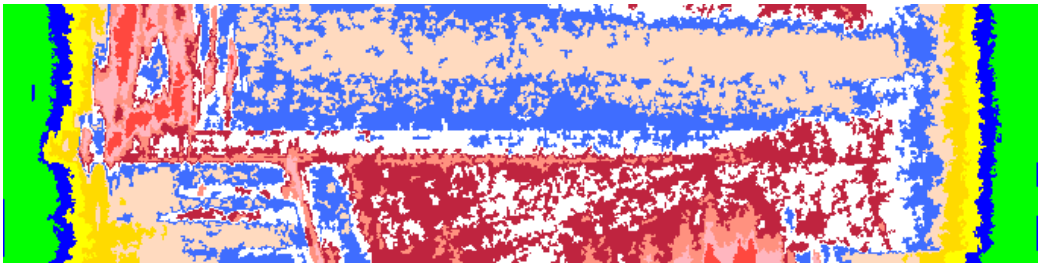

Figure 4: Regions extracted from the original radar image.

Figure 5: Three channels of noise used to simulate an image.

blend regions smaller than 32 pixels into their most appropriate neighbors. This process found 11 regions in the image, of which 4 are used in characterizing the intensity roll-off at each edge of the image in the range direction. For each region, the average Mueller matrix was calculated from the original single look data. These regions are shown in Figure 4.

For a test of the simulation, these regions and the Mueller matrices extracted from them were used to reconstruct the radar image using the algorithm described in this paper Three complex numbers of white Gaussian noise are generated for each pixel, as represented in Figure 5. These Gaussian noise numbers are multiplied by the appropriate eigenvalues and eigenvectors for the regions shown in Figure 4 according to (16) to create the simulated image. The resulting simulation is shown in Figure 6. While the fading for individual regions defined in Figure 4 is polarimetrically Rayleigh, the fading for the trees, fields and shadows, is non-Rayleigh as described by the polarimetric equivalent to (7), since each of these clutter areas are composed of several regions.

The match between the simulated image and the original image is very good overall, but the simulation is not an exact re-creation of the image in Figure 2. On a pixel by pixel basis, the original image and the simulated image are very different. But on a statistical basis, the two agree very closely, even for polarimetric quantities like co-polarized phase differences. One other way in which the original image and the simulated image differ is in the sensor artifacts: in the original image several streaks exist in range, due to very large scatterers at the same azimuth position but just off to the left of the image. These streaks apparently do not obey Rayleigh statistics and thus are not simulated faithfully. Sensor degradation post-processing is required to properly create these image artifacts.

In a sense, this exercise results in a lossy compression of the full polarimetric image down to a simple bitmap and 110 real numbers (11 Mueller matrices with 10 independent numbers each). While the original and the simulated image match closely in their amplitude distributions, there is no guarantee that either image has the correct image intensity. That is, if there were any calibration errors in the original image given by Figure 2, the errors have been simulated in Figure 6 as well.

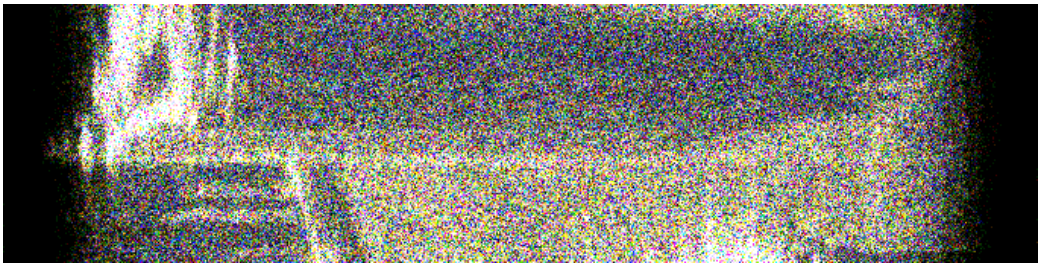

Figure 6: The simulated image generated from the noise in Figure 5 and the average Mueller matrices associated with each region in Figure 4.

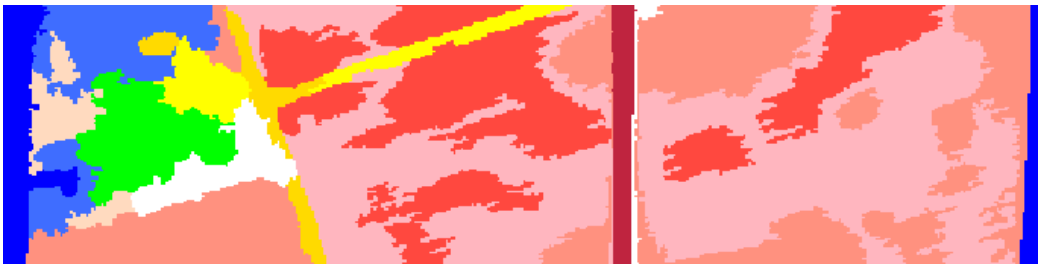

Figure 7: Regions extracted from the aerial photograph.

5.2. Simulation from Aerial Photography

As an additional example of the simulation algorithm, the aerial photograph of Figure 3 was used as the basis for generating the regions to be filled with clutter. The segmentation of the photograph into regions is shown in Figure 7. Using these regions, and the same averaged Mueller matrices as used in the previous simulation, the image in Figure 8 is simulated. A striking difference between the actual image of Figure 2 and this simulation is observed: the trees do not cast shadows in this simulation. This is because the aerial photograph was from overhead, while the original image was taken from near grazing. Built into the simulator is the ability to add shadows to simulated images. This is particularly useful when an image is to be simulated from another image taken at a different depression angle. In this case, the simulator can determine the heights of objects in the original image based on the shadows they cast and add the proper shadows to the new simulated image.

In a recent research effort conducted at The University of Michigan [30], a new technique for determining the extinction rate through a tree canopy from the measured radar backscatter response was developed. The technique is being applied now to all tree canopy data measured by the University of Michigan and the computed extinction rates will be incorporated into the MMW Clutter Database. The simulator will be able then to use the extinction rates and Mueller matrices of trees to simulate more realistic shadows.

5.3. Simulation from Ka-band to W-band

A third example of a simulated image addresses the problem of translating a SAR scene observed at one frequency to a SAR scene at a different frequency. For this simulation, the regions are determined from the original SAR image as depicted in Figure 4, but the Mueller matrices were extracted from the University of Michigan Clutter Database. For the

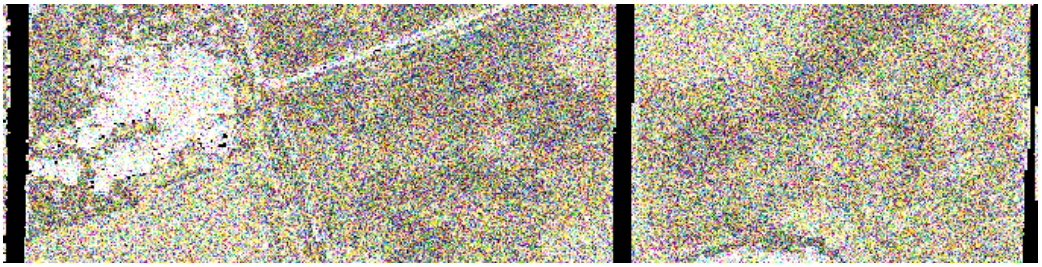

Figure 8: Simulated Ka-band image using the aerial photograph to determine the regions and the actual radar image to determine the Mueller matrices. Because the aerial photo was from directly overhead, the layout of the fields are correct, but the trees do not cast long shadows.

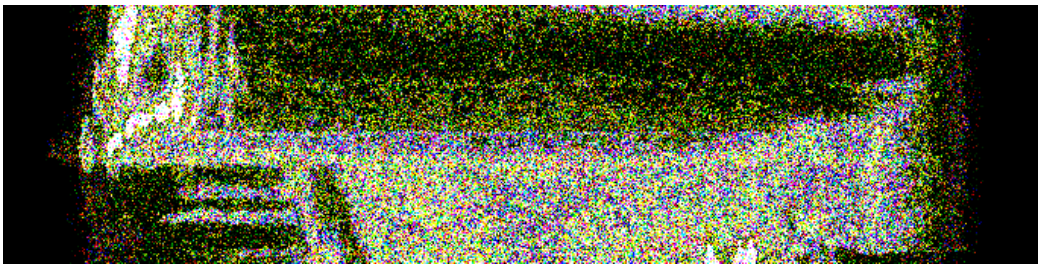

Figure 9: Simulated W-band image using the actual Ka-band radar image to determine the regions and Mueller matrices from the University of Michigan's phenomenology program.

shadow regions, the Mueller matrices for the trees were simply scaled down by a factor ranging between 2 and 10. The resulting simulation appears in Figure 9.

6. CONCLUSIONS

This paper introduces SPRI: the Simulator of Polarimetric Radar Images. SPRI is a radar simulator which can create high-resolution polarimetric single-look clutter images. The simulator draws on a user-specified geometry and a database of Mueller matrices for the regions within that geometry to create radar clutter images. The user-specified geometry may be from an existing SAR image at a different radar frequency from that desired, an existing aerial photograph, or the user's imagination.

For realistic simulations, the University of Michigan has constructed an online database of fully polarimetric measurements of clutter at 35 and 95 GHz. As of January 2001, this Clutter Database contains over 3500 Mueller matrices of terrain clutter, much of it near grazing incidence. Each Mueller matrix represents an average of many individual polarimetric backscatter measurements of a particular homogeneous clutter type. These measurements come from several sources: The University of Michigan's ultra-fast wide-band radars specifically designed for this project, an earlier generation network-analyzer based radars, the U. S. Army Research Laboratory's 95 GHz monopulse radar, and the University of Massachusetts' pulse radars.

This paper demonstrates that a Rayleigh fading simulator is sufficient for simulating most clutter, even those exhibiting texture and other heterogeneities.

REFERENCES

[1] S. Mallendant and M. Le Goff, "MELROS simulateur de fouillis de sol," in *Proceedings,* Low Grazing Angle Clutter: Its Characterization, Measurement and Application, Laurel, MD, 25–27 April 2000, NATO Sensors and Electronic Technology Panel (SET).

[2] F. W. Leberl, *Radargrammetric Image Processing,* Artech House, Norwood, MA, 1990.

[3] J. K. E. Tunaley, E. H. Buller, K. H. Wu, and M. T. Rey, "The simulation of the SAR image of a ship wake," *IEEE Transactions on Geoscience and Remote Sensing,* vol. 29, no. 1, pp. 149–156, January 1991.

[4] F. T. Ulaby and M. C. Dobson, *Handbook of Radar Scattering Statistics for Terrain,* Artech House, Norwood, MA, 1989.

[5] T. F. Haddock and F. T. Ulaby, "Millimeter-wave radar scattering from terrain: Data handbook," Technical Report 026247-1-T, The University of Michigan, Ann Arbor, MI, January 1990.

[6] F. Ulaby, R. McIntosh, and W. Flood, "Handbook of millimeter-wave polarimetric radar response of terrain," Joint technical report, The University of Michigan and the University of Massachusetts, March 1995.

[7] A. V. Saylor, "Comparisons of W-band clutter statistics," Letter Report RD-SS-99-03, Simulation Technologies, Inc., Huntsville, AL, 15March 1999.

[8] A. V. Saylor, "Documentation of Ka-band clutter statistics and model comparisons," Letter Report RD-SS-97-19, Simulation Technologies, Inc., Huntsville, AL, 15January 1997.

[9] R. Wellman, G. Goldman, J. Silvious, and D. Hutchins, "Analyses of millimeter wave radar low-angle ground-clutter measurements for European-like and desert environments," Technical Report ARL-TR-1102, US Army Research Laboratory, Adelphi, MD, July 1996.

[10] J. B. Billingsley, "Ground clutter measurements for surface-sited radar," Technical Report 786 rev. 1, Lincoln Laboratory, Lexington, MA, 1 February 1993.

[11] R. D. De Roo, F. T. Ulaby, A. E. B. El-Rouby, and A. Y. Nashashibi, "MMW radar scattering statistics of terrain at near grazing incidence," *IEEE Transactions on Aerospace and Electronic Systems,* vol. 35, no. 3, pp. 1010–1018, July 1999.

[12] F. T. Ulaby and E. C. Elachi, *Radar Polarimetry for Geoscience Applications,* Artech House, Norwood, MA, 1990.

[13] F. T. Ulaby, R. K. Moore, and A. K. Fung, *Microwave Remote Sensing: Active and Passive,* volume 2, Addison-Wesley, Reading, MA, 1982.

[14] D. J. Lewinski, "Nonstationary probabilistic target and clutter scattering models," *IEEE Transactions on Antennas and Propagation,* vol. 31, no. 3, pp. 490–498, May 1983.

[15] J. P. Welsh, "Smart weapons operability enhancement (SWOE) joint test and evaluation (JT&E) program final report," Technical Report SWOE Report 94-10, US Department of Defense, August 1994.

[16] A. Y. Nashashibi, K. Sarabandi, P. Frantzis, R. D. De Roo, and F. T. Ulaby, "A novel design of an ultra-fast wideband polarimetric radar," in *Digest*, IEEE Antennas and Propagation Society International Symposium, Orlando, FL, 11–15 July 1999. Invited Paper.

[17] F. T. Ulaby, T. F. Haddock, J. R. East, and M. W. Whitt, "A millimeterwave network analyzer based scatterometer," *IEEE Transactions on Geoscience and Remote Sensing*, vol. 26, no. 1, pp. 75–81, January 1988.

[18] R. J. Wellman, J. Nemarich, H. Dropkin, D. R. Hutchins, J. L. Silvious, and D. A. Wikner, "Polarimetric monopulse radar scattering measurements of targets at 95 GHz," in *Target and Clutter Scattering and their Effects on Military Radar Performance*, volume 501 of *AGARD Conference Proceedings*, pp. 30–1–30–13, Ottawa, ON, September 1991.

[19] R. F. van der Lans, *Introduction to SQL*, Addison-Wesley, Reading, MA, second edition, 1993.

[20] R. J. Yarger, G. Reese, and T. King, *MySQL and mSQL*, O'Reilly and Associates, Sebastopol, CA, first edition, 1999.

[21] J. S. Lee, M. R. Grunes, and R. Kwok, "Classification of multi-look polarimetric SAR imagery based on complex Wishart distribution," *International Journal of Remote Sensing*, vol. 15, no. 11, pp. 2299–2311, 20 July 1994.

[22] N. R. Goodman, "Statistical analysis based on a certain multivariate complex Gaussian distribution (an introduction)," *Annals of Mathematical Statistics*, vol. 34, pp. 152–177, 1963.

[23] J. L. Goldberg, *Matrix Theory with Applications*, McGraw-Hill, New York, 1991.

[24] A. M. Law and W. D. Kelton, *Simulation Modeling and Analysis*, McGraw-Hill, New York, 1982.

[25] S. C. Crocker and P. M. Witt, "Lincoln Laboratory 33.6 GHz SAR calibration overview," *Proceedings of SPIE*, vol. 1630, pp. 64–75, 1992.

[26] J. C. Henry, T. J. Murphy, and K. M. Carusone, "The Lincoln Laboratory millimeter-wave synthetic aperture radar SAR imaging system," *Proceedings of SPIE*, vol. 1630, pp. 35–52, 1992.

[27] F. T. Ulaby, R. K. Moore, and A. K. Fung, *Microwave Remote Sensing: Active and Passive*, volume 3, pp. 1818–1819, Artech House, Norwood, MA, 1986.

[28] A. Lopes, R. Touzi, and E. Nezry, "Adaptive speckle filters and scene heterogeneity," *IEEE Transactions on Geoscience and Remote Sensing*, vol. 28, no. 6, pp. 992–1000, November 1990.

[29] J. T. Tou and R. C. Gonzalez, *Pattern Recognition Principles*, Addison-Wesley, Reading, MA, 1974.

[30] A. Y. Nashashibi, F. T. Ulaby, P. Frantzis, and R. D. De Roo, "MMW measurements of the extinction and volume backscattering coefficients of tree canopies at near grazing incidence," in *Proceedings*, Low Grazing Angle Clutter: Its Characterization, Measurement and Application, Laurel, MD, 25–27 April 2000, NATO Sensors and Electronic Technology Panel (SET).